Structure of Regenerated Cellulose Films from Cellulose/Aqueous NaOH Solution as a Function of Coagulation Conditions

Guang YANG,[1,††] Hitomi MIYAMOTO,[2] Chihiro YAMANE,[2,†] and Kunihiko OKAJIMA[3]

[1]Department of Forest and Forest Products Sciences, Kyushu University,
6-10-1 Hakozaki, Higashi-ku, Fukuoka 812-8581, Japan
[2]Faculty of Home Economics, Kobe Women's University,
2-1 Aoyama, Higashisuma, Suma-ku, Kobe 654-8585, Japan
[3]Faculty of Engineering, Tokushima Bunri University, 1314 Shido, Sanuki 769-2193, Japan

ABSTRACT: The structure of regenerated cellulose films from cellulose/aqueous sodium hydroxide solution, prepared by coagulation of aqueous sulfuric acid, was investigated by X-ray diffraction and viscoelastic measurements. The X-ray crystallinity X_c and apparent crystal size decreased monotonically with increasing sulfuric acid concentration C_{sa} and an abrupt decrease was seen at $C_{sa} \geq 60$ wt %. In the viscoelastic measurements, four kinds of dynamic absorption peaks or shoulders were observed, named α_1, α_{sh}, β_a and γ, in order of decreasing temperature. The peak temperature of the α_1 absorption, $T_{max}\alpha_1$, decreased with increasing C_{sa}; conversely, $T_{max}\beta_a$ increased. This implies that there are two different kinds of amorphous regions. The activation energy of the β_a absorption also increased with increasing C_{sa}, as in the case of $T_{max}\beta_a$. In other words, concentrated sulfuric acid, which can dissolve cellulose, strengthens interactions between cellulose molecules in the amorphous region expressed by the β_a absorption. The tensile strength of these cellulose films showed a sudden decrease at $X_c < 25\%$. Micro-crystals possibly acted as crosslinking points, resulting in keeping tensile strength. In addition, the amorphous also greatly affected tensile strength; desirable amorphous structures for good properties were large and homogeneous amorphous units, which was expected to reduce stress concentration in the films. [doi:10.1295/polymj.PJ2006025]
KEY WORDS Cellulose / Alkali-Soluble / Coagulation / NaOH Solution / Structure / Hydrophobic / Hydrophilic /

Since Schweitzer's discovery of aq. cuprammonium hydroxide as a solvent for cellulose as early as 1857, hundreds of solvents have been discovered. Because most of these solvents are organic compounds with many compositions, aq. sodium hydroxide can be classified as one of the most simple and environmentally friendly solvents for cellulose. Although it has recently been reported that cellulose dissolves in water under supercritical conditions or using specially designed equipment,[1,2] aq. NaOH is still the simplest, safest and most practical solvent from the viewpoint of industrial feasibility. Environmental problems (*e.g.*, release of toxic gas, recovery of heavy metals and organic compounds) arising from commercially used cellulose solutions such as Viscose, cuprammonium hydroxide and *N*-methyl morpholine *N*-oxide, have created a demand for pollution-free solvents such as aq. NaOH. Cellulose dissolved in aq. NaOH is relatively safe environmentally, and can therefore be expected to engender few legal problems in this regard.

Numerous studies have been conducted by the research group of Asahi Chemical Industries on alkali-soluble cellulose, especially in aq. NaOH solution, and have yielded the following results: (1) the degree of intra-molecular hydrogen bonds in cellulose molecules controls the solubility of cellulose in aq. NaOH;[3] (2) the steam explosion process effectively breaks these hydrogen bonds;[4] (3) only aq. NaOH of specific concentration with specific structure can dissolve cellulose;[5] (4) cellulose dissolves molecularly in aq. NaOH;[6] and (5) regenerated cellulose fiber from aq. NaOH solution has the same mechanical properties as do commercially available regenerated cellulose fibers.[7] From a technical viewpoint, production facilities, including fully automated steam explosion apparatus, for manufacture of food materials from cellulose/aq. NaOH solution have already been constructed, and CEKICEL© from these facilities has been produced on a commercial scale. Moreover, the authors have made fibers with good mechanical properties for textile use in a bench-scale pilot plant. Although a large number of similar scientific and technological studies have been conducted, little is

---

†To whom correspondence should be addressed (E-mail: yamane@suma.kobe-wu.ac.jp).
††Present address: College of Life Science & Technology, Huazhong University of Science & Technology, Wuhan 430074, P. R. China Tel:86-27-63622057

known about the structure of the cellulose made from cellulose/aq. NaOH solutions. The only structural investigation that has been carried out is a comparison between this cellulose and commercially available regenerated cellulose fibers, such as Viscose Rayon, Bemberg© and Tencel©.[7]

The purpose of the study reported in this paper was to understand better a structure of the cellulose films prepared from cellulose/aq. NaOH solutions under various coagulation conditions. In addition, the effect of the structure on mechanical properties was also investigated, and the most desirable structure for good mechanical properties is proposed.

EXPERIMENTAL

Preparation of Alkali-Soluble Regenerated Cellulose and its Films from aq. NaOH Solution

Regenerated cellulose from cuprammonium solution (Bemlise©: Asahi Kasei Co., Ltd.; degree of polymerization DP = 800) was hydrolyzed by 25% aq. H_2SO_4 at 40 °C for 15 min, then washed with water at 20 °C until pH = 7, followed by drying at room temperature. The viscosity average molecular weight M_v of the hydrolyzed Bemlise© was determined through eq 1[8] to be 5.85×10^4 (DP = 361) from its intrinsic viscosity in cadoxen solution at 25 °C:

$$[\eta] = 3.85 \times 10^{-2} M_v^{0.76} \text{ (cm}^3 \text{ g}^{-1}) \tag{1}$$

where $[\eta]$ and M_v are the limiting viscosity number in cadoxen (cadmium oxide:ethylenediamine:NaOH: H_2O = 5:29:1.4:166, w/w/w/w) and the weight-average molecular weight, respectively. 10 g of hydrolyzed Bemlise© (water content about 11%) was added into 140 g of 9.1 wt % aq. NaOH, pre-cooled to 4 °C, mixed by a high speed mixer (T.K. Robomics, Tokushu Kika Co., Ltd.) intermittently for 10 min, then centrifuged at 10,000 rpm for 1 h. The resulting 6 wt % cellulose solution was cast on a glass plate to a thickness of 0.5 mm and the glass plate was immersed gently for 1–20 min in aq. H_2SO_4 solutions (concentration C_{sa}, 20–70 wt %) controlled at −5 °C. For elucidation of the C_{sa} dependence, the coagulation temperature T_c = −5 °C and the coagulation time t_c = 5 min were utilized. Similarly the t_c dependence was examined at C_{sa} = 60 wt % and T_c = −5 °C. The coagulated films were washed thoroughly with water for 1 d at 20 °C. The films thus prepared were dried by placement on a stainless-steel plate at 105 °C for 10 min.

X-Ray Diffractometry

X-Ray diffraction patterns of regenerated cellulose films were measured by a reflection method and recorded on an X-ray diffraction apparatus with scintil-lation counter (Rotaflex Ru-200PL, Rigaku Denki Co. Ltd., Japan). Samples were cut into particle-like size under ca. 120 µm so as to erase the influence from the crystalline orientation of each sample. Crystallinity index X_c was estimated by peak areas responsible for (110), (1-10) and (020) planes, separated by the Lorentz-Gaussian peak separation method.

Apparent crystal size (ACS) was estimated through use of Scherrer's eq 2:[9]

$$ACS = (\kappa\lambda/(\cos\theta))/\mu \tag{2}$$

$$\mu = (B^2 - b^2)^{1/2} \tag{3}$$

where κ is an apparatus constant taken as 0.9; λ, the wavelength of the Cu Kα line (1.542 Å); θ, the Bragg angle; B, the angular width in radians corresponding to the half-intensity width of the peaks of the (020) and (110) planes in the diffraction patterns; and b, another apparatus constant (0.2°).

Viscoelastic Measurements

The viscoelastic properties, namely mechanical loss tangentδ (tan δ) versus temperature (T) curves, for the cellulose films were recorded on a viscoelastic spectrometer (Model SDM-5000, Seiko Denshi, Co. Ltd., Japan) under the following conditions: frequency (f), 10 Hz; heating rate, 10 °C/min; measuring interval, 1 °C/min; sample length, 20 mm; sample width, 5 mm; initial charge, 10 g/mm²; scanning temperature range, −150–350 °C. The apparent activation energy, ΔH_a, for relaxation peaks of the films obtained at different values of C_{sa} was determined from the frequency dependence of the peak temperature T_{max} in the tan δ vs. T curves, using eq 4:

$$\Delta H_a = -R \frac{d \ln f}{d(1/T_{max})} \tag{4}$$

where R is the gas constant. The frequencies (f) used in the determination of ΔH_a were 1, 2, 5, 10, 20 and 50 Hz.

Tensile Strength

Tensile strength of the films with size of 3 × 20 mm was measured using tension meter (FGS-50V-L, SHIMPO Co., Ltd) with following conditions: elongation speed, 20 mm/min.; humidity, 60%; temperature, 20 °C. Out of six measurements for the same sample, expect for the highest and lowest ones, the values of four measurements were averaged.
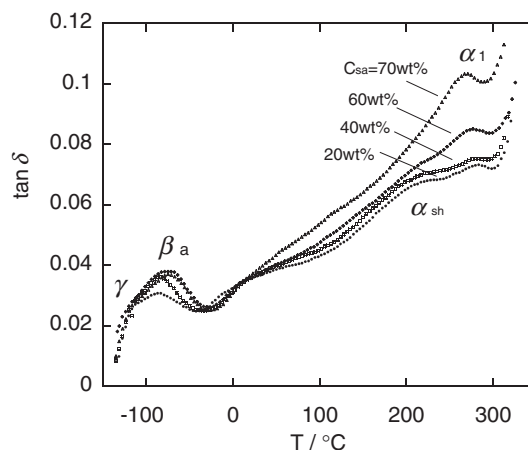
RESULTS AND DISCUSSION

Crystal parameters, crystallinity X_c and apparent crystal size ACS, are plotted against C_{sa} in Figure 1a, 1b. X_c decreased monotonically with increasing C_{sa} and rather sharply at $C_{sa} \geqq 60$ wt %. X_c of the films,
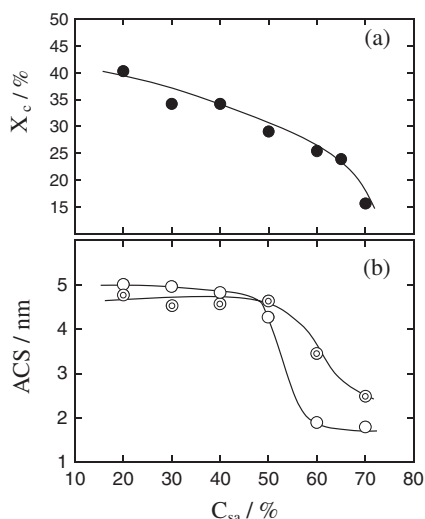
Figure 1. Effect of sulfuric acid concentration C_{sa} in coagulant on crystallinity X_c (a) and apparent crystal size ACS (b): ○, ACS of (110) crystal plane; ◎, ACS of (020) crystal plane; coagulation temperature T_c, $-5\,°C$; coagulation time t_c, 5 min.

Figure 2. Mechanical loss tangentδ ($\tan\delta$) - temperature (T) curves of cellulose films prepared by various C_{sa}; ○, $C_{sa} = 20$ wt %; □, 40 wt %; ●, 60 wt %; ▲, 70 wt %.
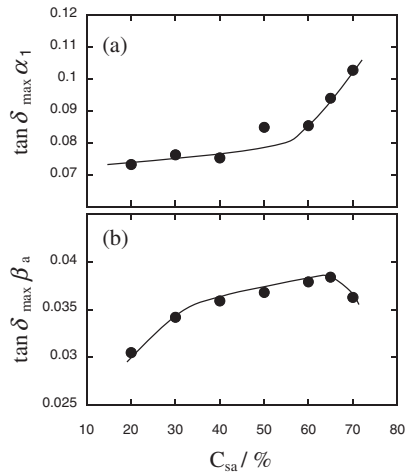
obtained by 20–60 wt % sulfuric acid coagulation, was *ca.* 25–40%, which was almost the same as for commercially available regenerated cellulose measured by the same method: viscose rayon, *ca.* 20–30%; cuprammonium rayon; *ca.* 30–40%; organic spun rayon (Tencel©), *ca.* 45%; and Cuprophane, *ca.* 40%.[7,10] X_c for cellulose from 70% sulfuric acid coagulation was under 15%. The value was very low for regenerated cellulose, and such a low value is only obtained by SO$_2$-amine solvent systems[11] or cellulose/concentrated sulfuric acid solution systems with coagulation at low temperature under 5 °C.[12] In other words, sulfuric acid coagulation made it possible to obtain cellulose with a wide range of X_c, from the lowest to the highest. This suggested that other structural parameters such as viscoelastic properties could also be closely controlled. ACS of the (110) and (020) planes also decreased with increasing C_{sa} and abrupt decreases were seen at $C_{sa} \geq 60$ wt %, where the sulfuric acid solution exhibits a dissolution ability for cellulose. The critical concentration necessary for dissolution is 57.5 wt %,[13] and the molecular ratio of sulfuric acid to water is 1:4 at this concentration. It is possible that only a specific composition of the solvent can dissolve cellulose as reported for the aq. NaOH solution system.[5] The report shows that total 8 mol of water solvate with a Na$^+$ ion and a OH$^-$ ion (*i.e.*, 4 mol/each ion) forming the cationic and anionic masses, respectively. The decrease in ACS of the (110) plane was much larger than that of (020) at $C_{sa} \geq 50$ wt %. This may have been caused by the difference in surface energies between the (020) and (110) crystal planes, whose surface energies are 110 mN m^{-1} and 101

mN m^{-1} respectively.[14] The low X_c and ACS are probably caused by coagulation followed by dissolution in concentrated sulfuric acid solution. However, there was almost no weight loss or decrease in degree of polymerization DP during the coagulation process, even under concentrated sulfuric acid condition such as $C_{sa} = 70$ wt %, $t_c = 5$ min., $T_c = -5\,°C$ because of the quite low temperature. Specifically, the DP of the sample was determined to be 352; the decrease in DP was only 2.5% from the initial value 361. In addition, previous report also shows that cellulose in concentrated sulfuric acid solution of which C_{sa} is over 60% and T_c is $-20\,°C$ retains its DP within 95% of the initial value after 24 h treatment.[13]

Figure 2 depicts typical $\tan\delta$ *vs. T* curves for films obtained at $C_{sa} = 20$, 40, 60 and 70 wt %. Four kinds of dynamic absorption peaks or shoulders, named α_1, α_{sh}, β_a and γ (in order of decreasing temperature), were observed with the exception of α_{sh} at $C_{sa} = 70$ wt %. Dynamic absorptions of regenerated cellulose are attributed to segmental motions as follows: α, micro-Brownian motion of cellulose main chain segments; β, local twisting motion of the main chain; and γ, rotational motion of the primary alcohol at the C$_6$ position around the C$_5$–C$_6$ axis.[15,16] In addition to these peaks, there seemed to be other peaks at around 0 °C and 100 °C. These may be "m" absorption and α_{H2O} absorption, which correspond to the melting point of H$_2$O and the cooperative motion of absorbed H$_2$O and polymer segment in an amorphous region respectively as described in the literature.[17] We do not discuss the γ absorption and the adsorptions at around 0 °C and 100 °C here because precise values of T_{max} and $\tan\delta_{max}$ could not be obtained from the figure; furthermore, the γ absorption obtained under these measuring conditions might be a transient signal

Figure 3. Effect of sulfuric acid concentration C_{sa} in coagulant on $\tan\delta_{max}\alpha_1$ (a) and $\tan\delta_{max}\beta_a$ (b): T_c, $-5\,°C$; t_c, 5 min.

Figure 4. Effect of sulfuric acid concentration C_{sa} in coagulant on $T_{max}\alpha_1$ (a) and $T_{max}\beta_a$ (b): T_c, $-5\,°C$; t_c, 5 min.
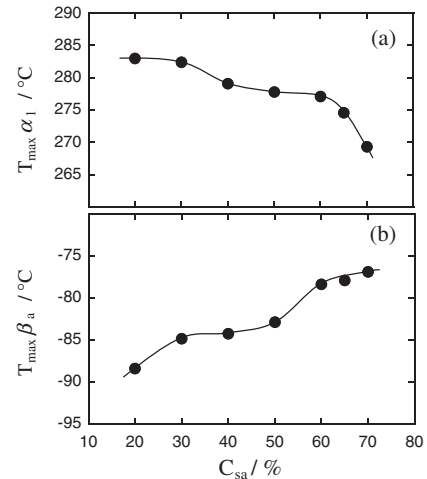
from the early stages of measurement.

A remarkable feature observed in films obtained with $C_{sa} > 60$ wt% was that α_1 and α_{sh} merged into one relatively sharp peak. When we saw the width of the α absorption (including both α_1 and α_{sh}), the width seemed to decrease with increasing C_{sa}. These results suggested that the amorphous region obtained at higher values of C_{sa} became more homogeneous.

Figure 3a, 3b shows the C_{sa} dependence of the peak intensity of $\tan\delta$ for the α_1 absorption, $\tan\delta_{max}\alpha_1$ (a), and for the β_a absorption, $\tan\delta_{max}\beta_a$ (b). Both $\tan\delta_{max}\alpha_1$ and $\tan\delta_{max}\beta_a$ increased with increasing C_{sa} with the exception of $\tan\delta_{max}\beta_a$ at $C_{sa} = 70$ wt%. Because $\tan\delta_{max}$ qualitatively indicates the proportion of amorphous region, the increase in $\tan\delta_{max}$ corresponded to a decrease of X_c shown in Figure 1. The effect of C_{sa} on $\tan\delta_{max}\alpha_1$ was quite similar to that for X_c and ACS, showing a drastic change at $C_{sa} > 50$ wt%. In contrast, $\tan\delta_{max}\beta_a$ mostly changed at lower C_{sa}, increased slightly at higher C_{sa}, then decreased again at $C_{sa} = 70$ wt%.

Figure 4a, 4b shows the C_{sa} dependence of $T_{max}\alpha_1$ (a) and $T_{max}\beta_a$ (b). $T_{max}\alpha_1$ decreased with increasing C_{sa}, whereas $T_{max}\beta_a$ increased. The two peaks had an opposite tendency of the C_{sa} dependence. It should be noted that T_{max} is an indicator of next two factors: (1) intermolecular forces such as intermolecular hydrogen bond and van der Waals force and (2) molecular stiffness mainly affected by the degree of intramolecular hydrogen bond.

The changes in $T_{max}\alpha_1$ and $\tan\delta_{max}\alpha_1$, which were clearly quite comparable to those of X_c and ACS, could be reasonably explained as follows. The lowering in X_c and ACS with increasing C_{sa} inevitably resulted in an increase in the proportion of amorphous region as revealed by the change in $\tan\delta_{max}\alpha_1$, and

at the same time caused the breakdown of intermolecular and intramolecular hydrogen bonds as revealed by the decreases in T_{max} for the α_1 absorption. In other words, the formation of intermolecular and intramolecular hydrogen bonds must have been prevented by high concentrations of sulfuric acid. This lowered X_c, ACS, and $T_{max}\alpha_1$ and heightened $\tan\delta_{max}\alpha_1$. In this connection, a previous study[18] on the same films used here reported the effect of C_{sa} on the degree of intramorecular hydrogen bonds. From the report, the degree of O_3–O_5' intramolecular hydrogen bonds determind by CP/MAS ^{13}C NMR decreased steeply at $C_{sa} \geq 60$ wt%. This also explains the shift in $T_{max}\alpha_1$ towards lower temperature and the increase in $\tan\delta_{max}\alpha_1$. It is well known that intramolecular hydrogen bonds, O3–O5′ and O2–O6′ for cellulose I[19] and O3–O5′ for cellulose II,[20] exist in cellulose molecules. From these results, the amorphous region showing α_1 absorption seems to be affected mainly by hydrogen bonds.
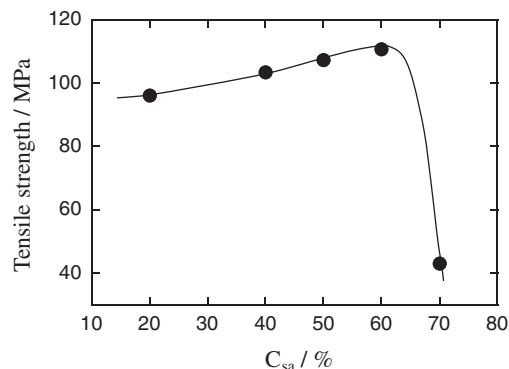
For the β_a relaxation the situation was somewhat different and more difficult to explain. That is, $T_{max}\beta_a$ increased by 15 °C with increasing C_{sa}, which suggests that intermolecular forces and molecular stiffness in the amorphous region which is defined by the β_a absorption increase with increasing C_{sa} in spite of the decrease in X_c and ACS. It is not clear what structural domain is the β_a absorption assigned to. However, if the structural domain is formed by hydrophobic interactions such as van der Waals forces, the effect of C_{sa} on $T_{max}\beta_a$ can be well explained because the structural domain probably becomes stable in the aqueous media (sulfuric acid solution) like a "micelle" in aqueous surfactant solution. The axial direction of the glucopyranose ring is thought to be hydrophobic because hydrogen atoms of C–H bonds are
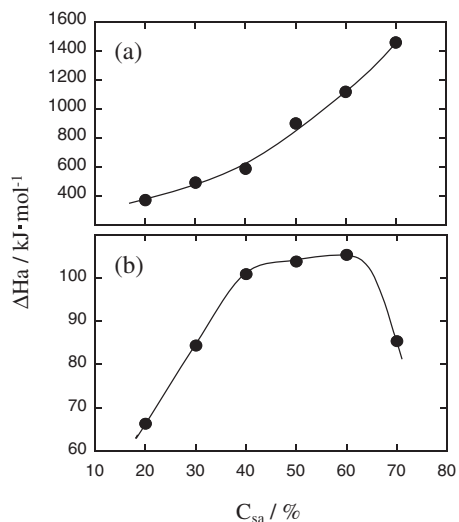
Figure 5. Effect of sulfuric acid concentration C_{sa} in coagulant on activation energy ΔH_a of α_1 absorption (a) and β_a absorption (b): T_c, $-5\,°C$; t_c, 5 min.

located on the axial position of the ring. Recently, hydrophobicity of the ring plane was proved to be very high by molecular mechanics simulation;[14] thus, cellulose molecules intrinsically have hydrophobic parts on the pyranose ring plane. Therefore, it is natural that these hydrophobic parts are combined together by van der Waals forces to form the structure which shows β_a absorption; Hayashi supports this possible structure as the basic and dominant features of regenerated cellulose, naming it Plane Lattice Structure or Sheet-like Structure[21] which is also depicted in other report.[14]

In order to clarify the mechanisms of the α_1 and β_a absorptions, their frequency dependence was examined as a function of C_{sa}. ΔH_a was evaluated from the measuring frequency f and T_{max} using eq 4. The dependence of ΔH_a for α_1 and β_a on C_{sa} is shown in Figure 5a, 5b. ΔH_a increased monotonically with increasing C_{sa} for α_1, with a rather high rate of increase at $C_{sa} \geqq 40\,\mathrm{wt\,\%}$. ΔH_a for β_a increased steeply until $C_{sa} = 40\,\mathrm{wt\,\%}$, then leveling off, and finally decreasing abruptly at $C_{sa} = 70\,\mathrm{wt\,\%}$. In general, ΔH_a values with a higher T_{max} are larger than those with a lower T_{max} because ΔH_a is governed by intermolecular forces, molecular stiffness and the size of the mobile unit. On the contrary, for the α_1 absorption, the higher ΔH_a at higher C_{sa} corresponded to a lower $T_{max}\alpha_1$. This indicated that the intermolecular interactions and molecular stiffness in this situation were weaker, and the size of the mobile unit yielding the absorption was larger, resulting in a higher $\tan\delta_{max}\alpha_1$ than that of samples coagulated at lower C_{sa}. The same result, *i.e.*, the higher ΔH_a showed the lower T_{max}, was reported for the regenerated cellulose prepared from a cuprammonium solution followed by
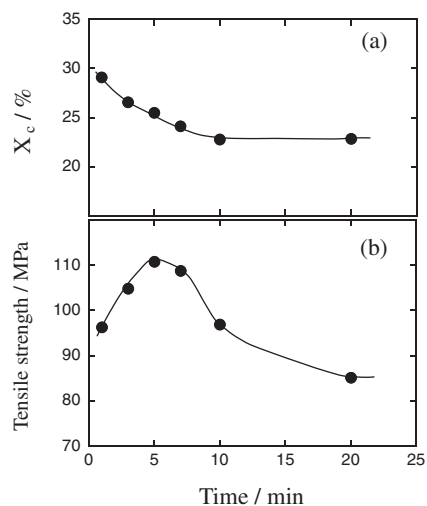
several coagulation systems.[17]

For α_1 absorption, $\tan\delta_{max}\alpha_1$ and ΔH_a increased but $T_{max}\alpha_1$ decreased with increasing in C_{sa}. In contrast, for β_a absorption, $\tan\delta_{max}\beta_a$, ΔH_a and $T_{max}\beta_a$ all increased with increasing in C_{sa}. These results imply that, (1) in the structural domain described by α_1 absorption, intermolecular forces mainly due to intermolecular hydrogen bond and molecular stiffness become weak, and size of amorphous region becomes large, (2) in the structural domain described by β_a absorption, intermolecular forces mainly due to hydrophobic interaction such as van der Waals forces and molecular stiffness become strong, and size of amorphous region becomes large with increasing in C_{sa}.

Figure 6 shows the relationship between tensile strength of the films and C_{sa} at a constant coagulation time of 5 min. The tensile strength increased with increasing C_{sa}, but decreased sharply at $C_{sa} = 70\,\mathrm{wt\,\%}$. Therefore, the tensile strength had a negative relation to X_c and ACS up to $C_{sa} = 60\,\mathrm{wt\,\%}$. Figure 7a, 7b

Figure 6. Effect of sulfuric acid concentration C_{sa} in coagulant on tensile strength of films: T_c, $-5\,°C$; t_c, 5 min.

Figure 7. Effect of coagulation time t_c on X_c (a) and tensile strength (b) of films: C_{sa}, 60 wt %; T_c, $-5\,°C$.
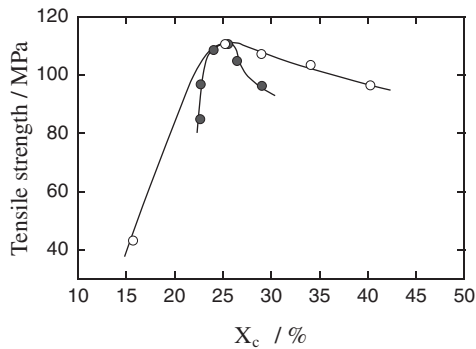
Figure 8. Effect of X_c on tensile strength of films: $\bigcirc$, constant t_c (5 min) and T_c ($-5\,^\circ$C) with different C_{sa} (20–70 wt %); $\bullet$, constant C_{sa} (60 wt %) and T_c ($-5\,^\circ$C) with different t_c (1–20 min).

shows X_c and tensile strength dependence on coagulation time at constant $C_{sa} = 60$ wt %. X_c decreased with increasing coagulation time and reached a plateau above 10 min. The tensile strength had a maximum at 5 min coagulation time. This also indicated the negative relation between the tensile strength and X_c up to 5 min. The tensile strengths of the films obtained under the two coagulation conditions, namely constant coagulation time with varying C_{sa} and constant C_{sa} with varying coagulation time, are plotted against X_c in Figure 8. Although there were some differences between the slopes of the lines in these two experimental systems, the lines depicted the same tendency, namely, X_c dependence of the tensile strength reversed at $X_c = 25\%$. In order to maintain tensile strength, a degree of crystallinity of *ca.* 25% or more must have been needed, producing an effect akin to crosslinking. Although the tensile strength of highly uniaxially oriented fibers is often very high even in the amorphous state, our films, whose molecular orientation relative to the stretching direction was random, probably required the minimum amount of crosslinkings. Micro-crystals, whose size are *ca.* 3 nm, in regenerated cellulose fibers, *e.g.*, viscose rayon and cuprammonium rayon exist side by side at 5–7 nm intervals in micro fibrils.[22] It would not be surprising in the structure if that micro-crystals acted as crosslinking points. The fact that the tensile strength rather decreased slightly with increasing X_c at $X_c \geq 25\%$ suggested that other structures such as amorphous domains or morphologies strongly affected the tensile strength at a far lower level of the theoretical strength.

It has been reported that coagulation at higher C_{sa} provided denser fine structures.[18] This is a possible reason for the strength dependence of cellulose on C_{sa}. In fiber production, another report indicated that the Young's modulus of their samples increased with increasing C_{sa} but decreased suddenly at $C_{sa} = 70\%$.[23]

This also closely resembles the strength dependence on C_{sa} shown in Figure 6. Although these two reports did not discuss the amorphous structure, this region probably affected the mechanical properties measured. In these amorphous structures, a higher $\tan \delta_{max}\alpha_1$ and ΔH_a of the α_1 relaxation resulted in higher tensile strength with one exception, namely when $C_{sa} = 70\%$ (Figures 3a, 5a and 6). This meant that the large size of amorphous units of cellulose main chains indicated by α_1 and α_{sh} probably increased tensile strength. In other word, this large amorphous region probably reduced stress concentration in the films, preventing the films from breaking. In addition, a homogeneous amorphous structure seemed to result in good mechanical properties because the narrow width of the α absorptions (including both α_1 and α_{sh}) also resulted in higher tensile strength.

Another amorphous factor, the β_a relaxation, possibly affected tensile strength. The C_{sa} dependences of $\tan \delta_{max}\beta_a$ and ΔH_a of the β_a relaxation (Figures 3b and 5b) closely paralleled the C_{sa} dependence of tensile strength (Figure 6). It was reasonable to suppose that a real mobile molecular unit at room temperature responsible for the β_a relaxation had a strong effect on the tensile strength at room temperature. Amorphous regions thus affected mechanical properties. Therefore, further research on such amorphous regions is necessary to clarify the key factors controlling real properties of polymers.

REFERENCES

1. M. Sasaki, T. Adschiri, and K. Arai, *J. Agric. Food Chem.*, **51**, 5376 (2003).
2. T. Kondo, *Cellul. Commun.*, **12**, 189 (2005).
3. K. Kamide, K. Okajima, and K. Kowsaka, *Polym. J.*, **24**, 71 (1992).
4. T. Yamashiki, T. Matsui, M. Saitoh, K. Okajima, K. Kamide, and T. Sawada, *Br. Polym. J.*, **22**, 73 (1990).
5. T. Yamashiki, K. Kamide, K. Okajima, K. Kowsaka, T. Matsui, and H. Fukase, *Polym. J.*, **20**, 447 (1988).
6. K. Kamide, M. Saito, and K. Kowsaka, *Polym. J.*, **19**, 1173 (1987).
7. C. Yamane, M. Mori, M. Saito, and K. Okajima, *Polym. J.*, **28**, 1039 (1996).
8. W. Brown and R. Wikstrom, *Eur. Polym. J.*, **1**, 1 (1965).
9. P. Schemer, *Gottinger Nachr.*, **2**, 98 (1918).
10. T. Hongo, C. Yamane, M. Saito, and K. Okajima, *Polym. J.*, **28**, 769 (1996).
11. A. Isogai and R. H. Atalla, *J. Polym. Sci., Part A: Polym. Chem.*, **29**, 113 (1991).
12. H. Ono, Y. Shimaya, T. Hongo, and C. Yamane, *Materials Research Society of Japan*, **26**, 569 (2001).
13. S. Takasu and K. Nishiyama, Japan Applied Patent, application number H4-357288, 1992.
14. C. Yamane, T. Aoyagi, and K. Okajima, *Polym. J.*, **38**, 819 (2006).

15. S. Manabe and R. Fujioka, *Carbohydr. Polym.*, **41**, 75 (2000).

16. S. A. Bradley and S. H. Carr, *J. Polym. Sci., Polym. Phys. Ed.*, **14**, 111 (1976).

17. S. Manabe and R. Fujioka, *Polym. J.*, **28**, 860 (1996).

18. T. Matsui, T. Sano, C. Yamane, K. Kamide, and K. Okajima, *Polym. J.*, **27**, 797 (1995).

19. Y. Nishiyama, P. Langan, and H. Chanzy, *J. Am. Chem. Soc.*, **124**, 9074 (2002).

20. P. Langan, Y. Nishiyama, and H. Chanzy, *J. Am. Chem. Soc.*, **121**, 9940 (1999).

21. J. Hayashi, J. Masuda, and Y. Watanabe, *Nippon Kagaku Kaisi*, **5**, 948 (1974).

22. C. Yamane, H. Ono, M. Saito, and K. Okajima, *Sen-I Gakkaishi*, **53**, 321 (1997).

23. C. Yamane, M. Saito, and K. Okajima, *Sen-I Gakkaishi*, **52**, 369 (1996).